Urea-Containing Mesoporous Silica for the Adsorption of Fe(III) Cations

Miriam Benitez,[†] Debasish Das,[†] Rita Ferreira,[‡] Uwe Pischel,*[,†] and Hermenegildo García*[,†]

Instituto de Tecnología Química/Departamento de Química, Universidad Politécnica de Valencia, Av. de los Naranjos s/n, E-46022 Valencia, Spain, and ESTG-Instituto Politécnico de Viana do Castelo, Av. do Atlântico, 4900-348 Viana do Castelo, Portugal

Received June 2, 2006. Revised Manuscript Received August 18, 2006

A urea-containing mesoporous silica with intraframework urea groups (UreaMS) was synthesized via a surfactant-templated route by co-condensation of an organosilane precursor and tetraethoxysilane. The material possesses hexagonal pores with a high degree of uniformity and shows long-range order as confirmed by the measurement of powder X-ray diffraction and N_2 adsorption isotherms. A detailed characterization by chemical analysis, ^{29}Si MAS NMR, X-ray photoelectron spectroscopy, thermogravimetric analysis, and FT-IR spectroscopy confirmed the integrity of urea groups inside the walls of the material. The results revealed a density of one urea group per ca. 13−16 silicon atoms. The efficiency of UreaMS for the adsorption of Fe(III) cations was tested. A distribution coefficient of $K_d = 700$ mL g^{-1} and an adsorption capacity of 0.19 mmol g^{-1} were determined. X-ray photoelectron spectroscopy confirmed the conservation of the oxidation state +3 for the iron within the mesoporous silica material.

Introduction

Recently, silica-based mesoporous organic−inorganic hybrid materials have been the focus of materials research.[1−4] The methods used to integrate organic functionalities into siliceous mesoporous matrixes can be classified as follows: (a) simple adsorption of an organic guest by a mesoporous silica, (b) postsynthetic modification, e.g., grafting of organic rests onto the walls of a mesoporous material, (c) co-condensation of a silicon precursor like tetraethoxysilane (TEOS) with a mono- or bis-organosilane [e.g., $R-Si(OEt)_3$ or $(OEt)_3Si-R-Si(OEt)_3$], and (d) condensation of a single-source bis-organosilane (e.g., $(OEt)_3Si-R-Si(OEt)_3$) precursor, yielding to periodically mesoporous organosilica (PMO).[3,4] Methods (a) and (b) lead often to an inhomogeneous distribution of the organic groups in the material and to blocking of the pores. The latter is a serious problem if the implemented organic function is used to interact with an analyte. The use of bis-organosilanes, with TEOS [method(c)] or as single-source precursors [method(d)], leads to an integration of the organic content in the materials framework, surpassing the problem of the pore blockage. Furthermore, PMO materials prepared by method (d) are characterized by a high loading and homogeneous distribution of the organic residues.

The preparation of PMOs has opened an elegant route to tailored functional materials via variation of organic residues R, ranging from alkyl and aromatic bridges[5−14] to more complex organic functions like heterocycles.[15,16] One of the drawbacks of PMOs is that not all bis-organosilanes can be templated to create periodic materials. The lack of rigidity of some organic precursors, which results in materials that do not maintain their shape after the surfactant template removal, solubility limitations, and an inappropriate hydrophobic/hydrophilic balance restrict the type of organic groups incorporated in PMOs.[17] An alternative synthetic procedure consists of co-condensation of the bis-organosilane with TEOS [method (c)]. General advantages of the co-condensation method include the economic use of the precious bis-organosilane, site isolation of the organic functions in the resulting material, and the wider applicability than the more restricted PMO approach. Thus, method (c) was used to synthesize mesoporous silicas, which incorporate rather complex organic moieties in the framework, such as photoactive chromophores[18,19] and chiral catalysts.[20,21] In these

* To whom correspondence should be addressed. E-mail: hgarcia@qim.upv.es (H.G.); upischel@itq.upv.es (U.P.).
[†] Universidad Politécnica de Valencia.
[‡] Instituto Politécnico de Viana do Castelo.

(1) Corriu, R. J. P. *Angew. Chem., Int. Ed.* **2000**, *39*, 1376−1398.
(2) Sayari, A.; Hamoudi, S. *Chem. Mater.* **2001**, *13*, 3151−3168.
(3) Hatton, B.; Landskron, K.; Whitnall, W.; Perovic, D.; Ozin, G. A. *Acc. Chem. Res.* **2005**, *38*, 305−312.
(4) Hoffmann, F.; Cornelius, M.; Morell, J.; Fröba, M. *Angew. Chem., Int. Ed.* **2006**, *45*, 3216−3251.
(5) Inagaki, S.; Guan, S.; Fukushima, Y.; Ohsuna, T.; Terasaki, O. *J. Am. Chem. Soc.* **1999**, *121*, 9611−9614.
(6) Melde, B. J.; Holland, B. T.; Blanford, C. F.; Stein, A. *Chem. Mater.* **1999**, *11*, 3302−3308.
(7) Yoshina-Ishii, C.; Asefa, T.; Coombs, N.; MacLachlan, M. J.; Ozin, G. A. *Chem. Commun.* **1999**, 2539−2540.
(8) Park, S. S.; Lee, C. H.; Cheon, J. H.; Park, D. H. *J. Mater. Chem.* **2001**, *11*, 3397−3403.
(9) Temtsin, G.; Asefa, T.; Bittner, S.; Ozin, G. A. *J. Mater. Chem.* **2001**, *11*, 3202−3206.
(10) Kuroki, M.; Asefa, T.; Whitnal, W.; Kruk, M.; Yoshina-Ishii, C.; Jaroniec, M.; Ozin, G. A. *J. Am. Chem. Soc.* **2002**, *124*, 13886−13895.
(11) Lee, B.; Luo, H.; Yuan, C. Y.; Lin, J. S.; Dai, S. *Chem. Commun.* **2004**, 240−241.
(12) Hunks, W. J.; Ozin, G. A. *J. Mater. Chem.* **2005**, *15*, 764−771.
(13) Landskron, K.; Ozin, G. A. *Angew. Chem., Int. Ed.* **2005**, *44*, 2107−2109.
(14) Liang, Y.; Hanzlik, M.; Anwander, R. *Chem. Commun.* **2005**, 525−527.
(15) Morell, J.; Wolter, G.; Fröba, M. *Chem. Mater.* **2005**, *17*, 804−808.
(16) Olkhovyk, O.; Jaroniec, M. *J. Am. Chem. Soc.* **2005**, *127*, 60−61.
(17) Burleigh, M. C.; Markowitz, M. A.; Spector, M. S.; Gaber, B. P. *Chem. Mater.* **2001**, *13*, 4760−4766.

10.1021/cm061287n CCC: $33.50
Published on Web 10/07/2006

examples site isolation and control of the density of the active organic component play a decisive role in the optimal performance of the material. The latter would suffer from undesired interactions among the implemented organic functions, due to high loading.

The potential of appropriately functionalized mesoporous materials in environmental applications, namely, for the adsorption of transition metal cations, has been realized very soon. Consequently, a large variety of materials with a metal binding motif hanging in the pore channel has been prepared by co-condensation of TEOS and mono-organosilanes precursors [e.g., $R-Si(OEt)_3$]. Thiols, thiourea, and amines have been used as metal ion binding motifs for the efficient removal of toxic heavy metals like Hg(II), Cu(II), and Cd(II).[22−25] Also, thiol- and amino-functionalized materials with larger pores than MCM-41 (e.g., SBA-15) have been successfully applied for removal of heavy-metal ions, e.g., Hg(II), Cu(II), and Zn(II).[26,27] However, the use of mesoporous organosilica with intraframework metal binding motifs has been explored to a lesser extent. Surfactant-templated co-condensation of TEOS with 1,4-bis[3-(trimethoxysilyl)-propyl]ethylenediamine yielded mesoporous materials for adsorption of Cu(II).[28,29] Effective Hg(II) adsorption was accomplished with mesoporous organosilica materials containing tetrasulfide or heterocyclic isocyanurate bridging groups.[16,30] Mesoporous organosilicas with cyclam units integrated into the wall and hanging in the pore channels have been used for Cu(II), Co(II), Eu(III), and Gd(III) complexation.[31−34] Further, a 4,5-dihydroimidazolium-derived PMO showed enhanced perrhenate anion adsorption.[35] Recently, PMOs with diphenyl ether or sulfide bridges in the channel walls have been reported, which are foreseen to be promising candidates for intraframework metal complexation.[36]

In the present work the preparation of a urea-containing mesoporous silica (UreaMS) and its use for adsorption of Fe(III) are reported. UreaMS combines the large surface area of a mesoporous material with the advantage of intraframework urea groups as metal-binding motifs, avoiding the problem of channel blocking by the organic function. The material was prepared by surfactant-templated co-condensation of TEOS and a urea-derived bis-organosilane and fully characterized by complementary methods, which revealed the integrity of the organic urea residue in the pore walls.

It is interesting to note that although Fe(III) is a nontoxic metal and does not constitute a threat to human health, its presence in drinking water is undesired. Already in a concentration as little as 0.3 mg L^{-1}, Fe(III) turns the water into a reddish-brown color and leaves stains on laundry, which are hard to remove. Therefore, iron in general is considered a secondary and aesthetic contaminant.

Experimental Section

Materials. 1,4-Diaminobutane, 3-isocyanatopropyltriethoxysilane, and tetraethoxysilane (TEOS) were obtained from Aldrich (>98%). $FeCl_3 \cdot 6H_2O$ was from Sigma. Cetyltrimethylammonium bromide (CTABr), which served as surfactant template in the synthesis of the mesoporous silica, was also purchased from Aldrich. All chemicals were used as received.

Synthesis of Urea-Derived Organosilane Compound (1). The urea-derived organosilane compound **1** was obtained as colorless solid by reacting neat 1,4-diaminobutane and 3-isocyanatopropyltriethoxysilane at room temperature. The reaction was followed by the disappearance of the characteristic IR signal for the isocyanate group at ca. 2250 cm^{-1}. $[(EtO)_3Si(CH_2)_3NHCONH]_2(CH_2)_4$. ^1H NMR (CD_3OD, 300 MHz): δ 3.77 (q, $J = 7.0$ Hz, 12H, CH_3CH_2O), 3.00−3.10 (m, 8H, CH_2N), 1.40−1.55 (m, 8H, CH_2), 1.17 (t, $J = 7.0$ Hz, 18H, CH_3CH_2O), 0.53−0.59 (m, 4H, $Si-CH_2$). ^{13}C NMR (CD_3OD, 75 MHz): δ 160.06 (C═O), 58.27 (CH_3CH_2O), 42.62 (CH_2N), 39.46 (CH_2N), 27.44 (CH_2), 23.55 (CH_2), 17.41 (CH_3CH_2O), 7.19 ($Si-CH_2$). IR (KBr): 2928 (CH_2), 1635 (ν_{CO}, amide I), 1591 (δ_{NH}, amide II) cm^{-1}. MS (ESI): *m/z* 583.3 ([M + 1]).

Synthesis of Urea-Containing Mesoporous Silica (UreaMS). UreaMS was obtained by using precursor **1** and TEOS as silicon sources in a surfactant-templated co-condensation under basic conditions, similar to previously reported methods (cf. Scheme 1).[19−21,37] The following experimental conditions applied: **1** and TEOS were mixed with a 20% aqueous ammonia solution, water, and CTABr. The initially formed gel was transferred into a polyethylene container and heated at 353 K for 4 days. To maximize the organic content of the resulting material, the ratio of TEOS/**1** was varied. However, only from batches with molar ratios higher than TEOS/**1** 95:5, crystalline materials with a sufficient stability upon removal of the template were obtained. In the case of a higher organic content, the material collapsed after removal of CTABr. A typical batch had the following composition (molar ratio): 5.0:95.0:114.0:8.0:0.13 **1**:TEOS:H_2O:NH_3(20%):CTABr. The template was removed by solvent extraction with *n*-heptane under acidic conditions (diluted hydrochloric acid). The obtained material was analyzed with regard to its organic and silicon content: C, 9.26%; N, 3.10%; Si, 40.10%.

(18) Álvaro, M.; Ferrer, B.; García, H.; Hashimoto, S.; Hiratsuka, M.; Asahi, T.; Masuhara, H. *ChemPhysChem* **2004**, *5*, 1058−1062.
(19) Álvaro, M.; Benitez, M.; Das, D.; Ferrer, B.; García, H. *Chem. Mater.* **2004**, *16*, 2222−2228.
(20) Baleizão, C.; Gigante, B.; Das, D.; Álvaro, M.; García, H.; Corma, A. *Chem. Commun.* **2003**, 1860−1861.
(21) Baleizão, C.; Gigante, B.; Das, D.; Álvaro, M.; García, H.; Corma, A. *J. Catal.* **2004**, *223*, 106−113.
(22) Brown, J.; Mercier, L.; Pinnavaia, T. J. *Chem. Commun.* **1999**, 69−70.
(23) Brown, J.; Richer, R.; Mercier, L. *Microporous Mesoporous Mater.* **2000**, *37*, 41−48.
(24) Lee, B.; Kim, Y.; Lee, H.; Yi, J. *Microporous Mesoporous Mater.* **2001**, *50*, 77−90.
(25) Antochshuk, V.; Jaroniec, M. *Chem. Commun.* **2002**, 258−259.
(26) Dai, S.; Burleigh, M. C.; Shin, Y.; Morrow, C. C.; Barnes, C. E.; Xue, Z. *Angew. Chem., Int. Ed.* **1999**, *38*, 1235−1239.
(27) Liu, A. M.; Hidajat, K.; Kawi, S.; Zhao, D. Y. *Chem. Commun.* **2000**, 1145−1146.
(28) Hossain, K. Z.; Mercier, L. *Adv. Mater.* **2002**, *14*, 1053−1056.
(29) Zhu, H.; Jones, D. J.; Zajac, J.; Dutartre, R.; Rhomari, M.; Rozière, J. *Chem. Mater.* **2002**, *14*, 4886−4894.
(30) Zhang, L.; Zhang, W.; Shi, J.; Hua, Z.; Li, Y.; Yan, J. *Chem. Commun.* **2003**, 210−211.
(31) Corriu, R. J. P.; Mehdi, A.; Reyé, C.; Thieuleux, C. *Chem. Commun.* **2002**, 1382−1383.
(32) Corriu, R. J. P.; Mehdi, A.; Reyé, C.; Thieuleux, C. *New J. Chem.* **2003**, *27*, 905−908.
(33) Corriu, R. J. P.; Mehdi, A.; Reyé, C.; Thieuleux, C. *Chem. Commun.* **2003**, 1564−1565.
(34) Corriu, R. J. P.; Mehdi, A.; Reyé, C.; Thieuleux, C.; Frenkel, A.; Gibaud, A. *New J. Chem.* **2004**, *28*, 156−160.
(35) Lee, B.; Im, H.-J.; Luo, H.; Hagaman, E. W.; Dai, S. *Langmuir* **2005**, *21*, 5372−5376.
(36) Hunks, W. J.; Ozin, G. A. *Chem. Commun.* **2004**, 2426−2427.
(37) Benitez, M.; Bringmann, G.; Dreyer, M.; García, H.; Ihmels, H.; Waidelich, M.; Wissel, K. *J. Org. Chem.* **2005**, *70*, 2315−2321.

Scheme 1

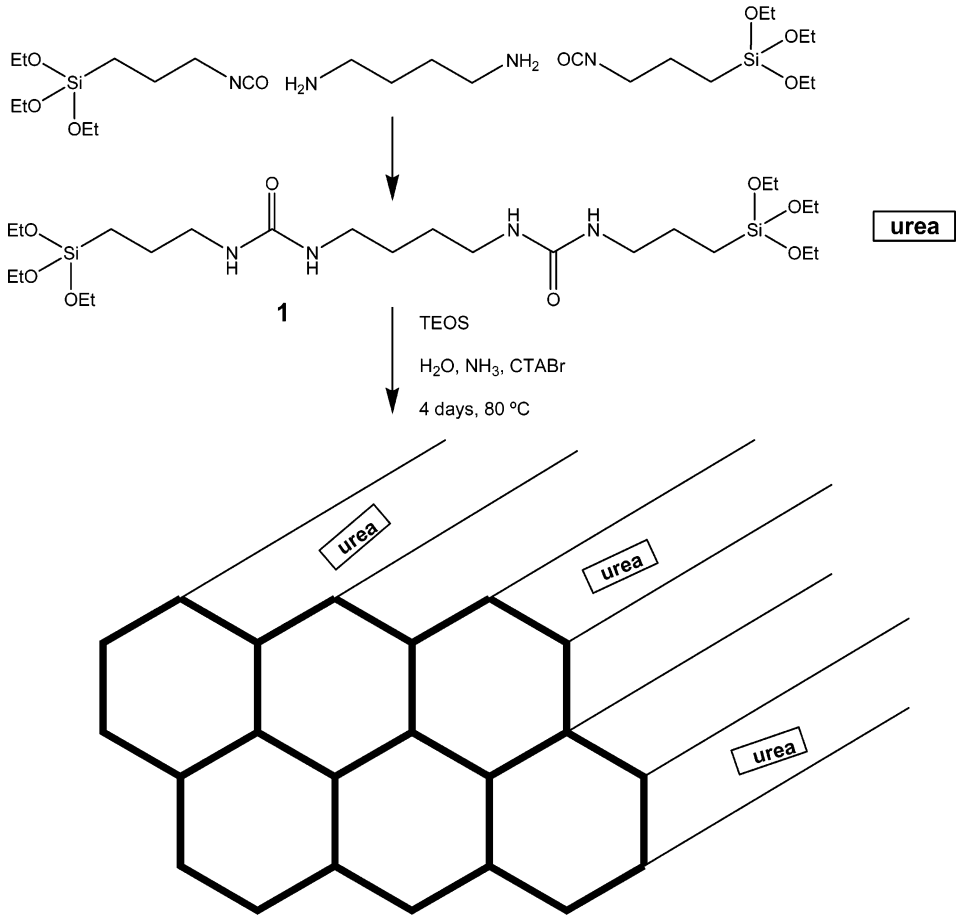

Test of Fe(III) Adsorption by UreaMS. The potential of UreaMS for Fe(III) adsorption was tested in a procedure similar to reported ones.[24,28,35] Fifty milligrams of UreaMS was suspended in 5 mL of a 0.48 mM solution of $FeCl_3 \cdot 6H_2O$ in water. This suspension was sonificated for 1 h, after which the solid was filtered off. The Fe(III) uptake was monitored by measuring the UV absorption at $\lambda_{max} = 295$ nm of the initial and final solution ($\epsilon_{295} = 2200\ M^{-1}\ cm^{-1}$, this work). The distribution coefficient (K_d) was determined using eq 1,[24,26,28,35]

$$K_d = (c_i - c_f)V_{soln}/(c_f m_{ads}) \quad (1)$$

with c_i as the initial metal ion concentration, c_f as the ion concentration after adsorption, V_{soln} as the volume of the solution (in mL), and m_{ads} as the amount of adsorbent (in g). UreaMS loaded with Fe(III) to its maximum capacity (Fe−UreaMS) was prepared in the following way: a suspension of 100 mg of UreaMS in 10 mL of a 40 mM aqueous solution of Fe(III) was stirred for 24 h. After this time the solid was filtered off and washed with copious amounts of water. After air-drying, a slightly yellowish material was obtained. Iron analysis of this material (Fe−UreaMS) was done by dissolving the solid in HF and performing atomic absorption spectrometry (AAS). An iron content of 10.4 mg (0.19 mmol) per 1 g of UreaMS was determined.

Materials Characterization. The ^1H and ^{13}C NMR spectra of precursor **1** were measured with a Bruker AV-300 spectrometer using d_4-methanol as solvent and tetramethylsilane (TMS) as internal standard. The infrared spectrum of **1** was recorded with a FT/IR-460 plus Jasco spectrometer. PXRD data were collected on a Phillips X'Pert diffractometer using Cu Kα radiation with $\lambda = 1.5406$ Å. Bragg−Brentano geometry was provided by a secondary graphite monochromator. N_2 adsorption isotherms were recorded at 77 K with a Micromeritics ASAP 2000 instrument. The specific surface area was determined by the BET (Brunnauer−Emmett−Teller) method and the pore size distribution by the BJH (Barrett−Joyner−Halenda) method using the desorption branch of the isotherm plot. ^{29}Si MAS NMR (magic angle spinning-nuclear magnetic resonance spectroscopy) of UreaMS was done on a Bruker 400 spectrometer with a zirconia rotor spinning at 5.5 kHz. Thermogravimetric analysis (TGA) was performed under air in the range of 298−1073 K (5 K min^{-1}) with a thermoanalyzer Netzsch STA 409 EP. FT-IR spectra of vacuum-degassed, self-supported pellets of the solid samples were recorded at 373 K with a Nicolet 710 FT spectrophotometer. X-ray photoelectron spectroscopy (XPS) of compressed pellets of the materials was performed with an ESCALAB 200A spectrometer using Mg Kα radiation. Binding energies were corrected to the binding energy of Si 2p (103.4 eV for SiO_2).[38] Additionally, UreaMS and Fe−UreaMS were analyzed by diffuse reflectance UV/vis spectroscopy of powder samples with a Varian Cary 5G UV/vis spectrophotometer.

Results and Discussion

Chemical Composition of UreaMS. Elemental analysis for carbon and nitrogen as indicators for the implemented organic functionality revealed ca. 1.1 mmol of urea groups per 1 g of UreaMS, which is in the same order of magnitude as for other functionalized materials designed for metal-ion adsorption.[22,25,27,33,39] The experimental C/N ratio (3.0) is

(38) Dane, A.; Demirok, U. K.; Aydinli, A.; Suzer, S. *J. Phys. Chem. B* **2006**, *110*, 1137−1140.
(39) Liu, C.; Lambert, J. B.; Fu, L. *J. Mater. Chem.* **2004**, *14*, 1303−1309.

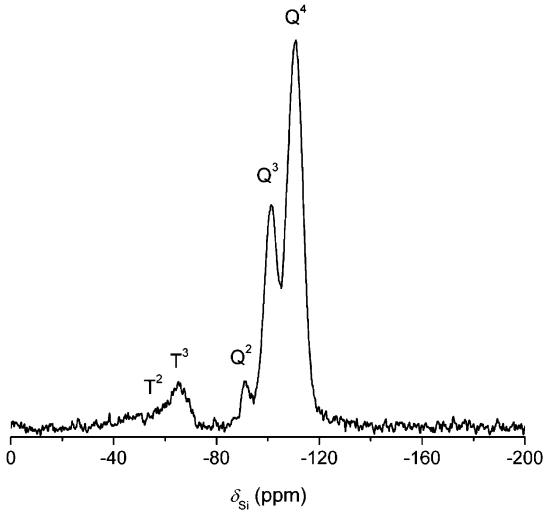

Figure 1. ^{29}Si MAS spectrum of UreaMS.

virtually the same as theoretically expected for the bis-urea residue (2.6).

The composition of the new material was further investigated by ^{29}Si MAS NMR spectroscopy. Two groups of signals can be distinguished in the spectrum (cf. Figure 1): (a) three Q signals from silicon atoms without organic substitution and (b) two T signals related to organo-substituted silicon. The Q signals at −91, −101, and −111 ppm were assigned to Q^2, Q^3, and Q^4 structures, respectively. The Q^4 signal, corresponding to fully condensed SiO_4, is clearly dominating (ca. 59% of all silicon atoms, obtained by signal integration), while the Q^3 signal caused by SiO_3OH groups corresponds to ca. 29% of all silicon atoms. The Q^2 signal, related to partially condensed $SiO_2(OH)_2$, contributes with only ca. 5%. The other signal group between −70 and −50 ppm consists of a T^3 structure element (peak at −65 ppm), i.e., organo-substituted silicon without uncondensed hydroxyl groups ($RSiO_3$), contributing with 4% to the total of silicon atoms.[8,29] Finally, a shoulder at −59 ppm (ca. 3%) was assigned to T^2 units ($RSiO_2OH$).[8,40] The integration of the signals indicates that UreaMS contains one uncondensed silanol group per ca. 3 silicon atoms and one urea group per ca. 14 silicon atoms. Based on the elemental analysis (cf. Experimental Section) of the material, a silicon/urea ratio of ca. 13 can be estimated, which is in excellent agreement with the result obtained by NMR spectroscopy.

UreaMS was further investigated by X-ray photoelectron spectroscopy (XPS) and the binding energies for C 1s and N 1s were determined (cf. Figure 2). For N 1s a binding energy of 399.9 eV was measured, which is in excellent agreement with the value for parent urea (399.9 eV).[41] As expected, based on the chemical composition of the material, the photoelectron spectra for C 1s contained more than one component. The single contributions were determined by deconvolution analysis using Gaussian functions. The fit was performed in such a way that the areas under the deconvoluted peaks agree well with the expected ratio of the different carbons (alkyl CH_2 and carbonyl C═O) according to the chemical structure of the organic moiety.[42,43] The resulting C 1s binding energies were 284.9 and 288.0 eV, which correspond to alkyl and carbonyl C atoms, respectively.[41,43] It is important to note that XPS is a surface analysis method and gives information about the relative content of the analyzed element up to ca. 50 Å depth. With use of the areas of the N 1s and Si 2p peaks, the density of urea groups within the silica framework was estimated as one urea group per ca. 16 silicon atoms. The good correlation between this result and the ratio obtained by elemental analysis ($n_{Si}/n_{urea} = 13$) and by ^{29}Si MAS NMR ($n_{Si}/n_{urea} = 14$) suggests that the urea groups are uniformly distributed between the exterior and the interior of the material. Based on these data as well as the structural characterization (see below), the formation of subdomains with enriched organic content is therefore rather unlikely.

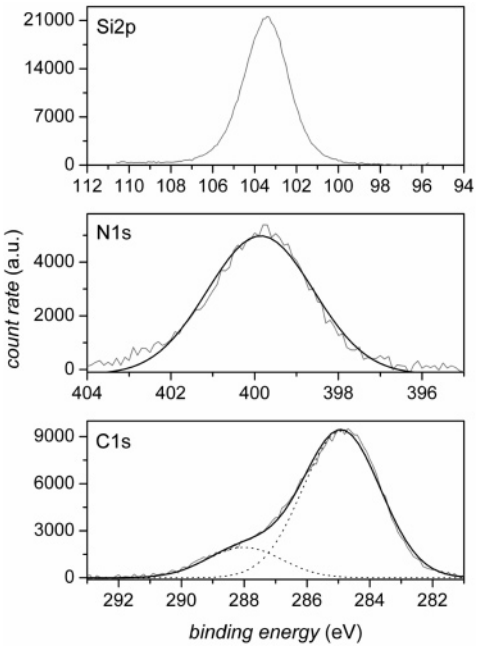

Figure 2. XPS graphs for Si 2p, N 1s, and C 1s for UreaMS and respective deconvolution fits based on Gaussian functions (dotted and full lines). The Si 2p is dominated (95%) by SiO_2, such that deconvolution was discarded.

The thermogravimetric profile of UreaMS is depicted in Figure 3. Upon heating under air, the material undergoes a total weight loss of 58%. The initial weight loss, until 393 K, was attributed to thermodesorption of water and corresponds to 37%. No significant weight loss (only ca. 4%) was observed in the corresponding thermal decomposition range of the surfactant (393−513 K), indicating a major removal of the template.[17,44,45] The decomposition of the organic components of the material occurred between 513 and 923 K, leading to a total weight loss of 17%. Presumably, the rather extended temperature range is caused by several

(40) Moreau, J. J. E.; Pichon, B. P.; Wong Chi Man, M.; Bied, C.; Pritzkow, H.; Bantignies, J.-L.; Dieudonné, P.; Sauvajol, J.-L. *Angew. Chem., Int. Ed.* **2004**, *43*, 203−206.
(41) Chen, T.-L.; Xiao, S.-X.; Li, P. *Int. J. Quant. Chem.* **1997**, *64*, 247−248.
(42) Defosse, C.; Friedman, R. M.; Fripiat, J. *Bull. Chim. Soc. France* **1975**, 1513−1518.
(43) Pradier, C.-M.; Salmain, M.; Zheng, L.; Jaouen, G. *Surf. Sci.* **2002**, *502*−*503*, 193−202.
(44) Kruk, M.; Jaroniec, M.; Guan, S.; Inagaki, S. *J. Phys. Chem. B* **2001**, *105*, 681−689.
(45) Hamoudi, S.; Kaliaguine, S. *Microporous Mesoporous Mater.* **2003**, *59*, 195−204.

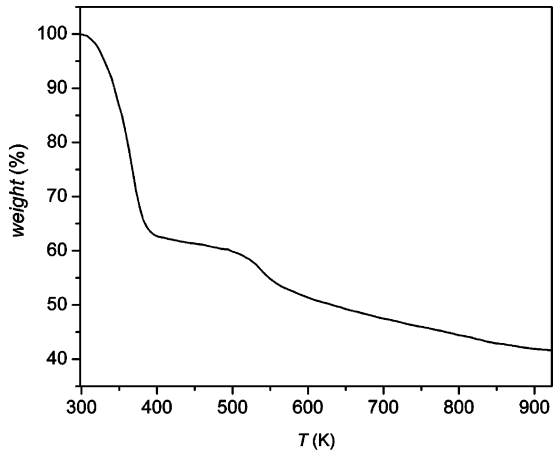

Figure 3. Thermogravimetric profile of UreaMS.

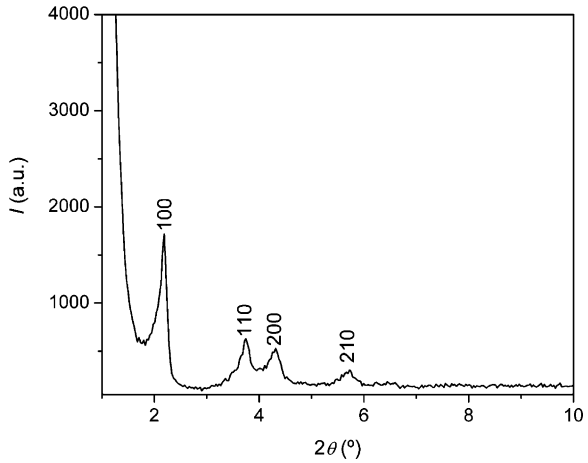

Figure 4. Powder X-ray diffraction pattern of UreaMS.

chemical reactions (e.g., urea decomposition, oxidation reactions, and "channel metamorphosis" via proton transfer from silanols to methylene groups).[46] Weight losses in a similar temperature range (573−923 K) were observed for ethylene-bridged PMOs.[44,45] Therefore, according to TGA, about 17 wt % of the UreaMS is due to the intraframework organic content of the material, corresponding to 1.3 mmol of urea units per 1 g of UreaMS (cf. result from elemental analysis).

Materials Structure and Porosity. The degree of structural order of UreaMS was investigated by powder X-ray diffraction (PXRD), as shown in Figure 4. The sharp peaks indicate long-range structural order. Moreover, the observation of characteristic (100), (110), and (200) peaks points to a hexagonal mesostructure, akin to MCM-41.[47] Furthermore, the XRD pattern exhibits a distinct signal assigned to the (210) reflection. This rarely observed signal suggests that UreaMS can be considered as ideally hexagonally ordered.[48] For such structures the ratio $d_{100}/d_{110} = \sqrt{3}$:1 is expected, which is also obeyed by the material. As-synthesized, UreaMS showed a sharp low-angle (100) peak at a spacing of $d_{100} = 41.2$ Å, while upon removal of the template by solvent extraction, a slightly lower spacing ($d_{100} = 40.4$ Å) and a hexagonal unit cell parameter of $a_0 = 46.6$ Å were obtained.

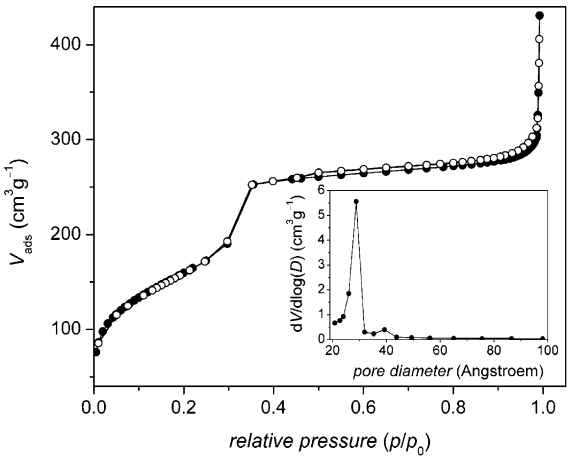

Figure 5. Nitrogen adsorption−desorption isotherms of UreaMS at 77 K. The inset shows the pore size distribution determined from the desorption branch of the isotherm.

To characterize UreaMS regarding its specific surface area and pore size distribution, isothermal nitrogen adsorption−desorption measurements were performed. The isotherm plot, shown in Figure 5, can be classified as type IV. The observation of an abrupt rise at 0.35 relative pressure due to capillary condensation indicates a uniform mesoporous structure,[49] characteristic of MCM-41.[47] The isotherm is also characterized by a small hysteresis loop in the range of p/p_0 of ca. 0.6−0.8, which is ascribed to the interparticle volume. The Brunnauer−Emmett−Teller (BET) specific surface area was obtained as 584 m^2 g^{-1}, and the Barrett−Joyner−Halenda (BJH) adsorption pore volume was estimated as 0.49 cm^3 g^{-1}. The pore diameter distribution was determined from the desorption branch of the isotherm, yielding an average pore size of 30 Å (cf. inset of Figure 5). The narrow size distribution confirms the uniformity of the porous structure. The thickness of the pore walls of UreaMS calculated by subtracting the internal average pore size (30 Å) from the spacing between the pores (a_0) is 16.6 Å.[50]

Adsorption of Fe(III) by UreaMS. An adsorption study with an initial Fe(III) quantity significantly lower than the number of theoretically available urea units yielded that 87% of the metal cation were adsorbed after 1 h of sonification (cf. Experimental Section). The adsorption capacity of UreaMS compares quite favorably with that of other mesoporous silicas used for the adsorption of Hg(II), Cu(II) cations, or ReO_4^- anions.[17,25,35] Application of eq 1 (cf. Experimental Section) led to a distribution coefficient of K_d = 700 mL g^{-1}. Similar values (K_d ca. 500−700 mL g^{-1}) were obtained for perrhenate anion adsorption in acidic media by a PMO with a 4,5-dihydroimidazolium-derived functionality.[35] Higher K_d values (5300−39000 mL g^{-1}) for some metal cations [e.g., Cu(II) and Hg(II)] have been reported using other functionalized mesoporous silicas.[26,28] The

(46) Asefa, T.; McLachlan, M. J.; Grondey, H.; Coombs, N.; Ozin, G. A. *Angew. Chem., Int. Ed.* **2000**, *39*, 1808−1811.
(47) Kruk, M.; Jaroniek, M.; Sakamoto, Y.; Terasaki, O.; Ryoo, R.; Ko, C. H. *J. Phys. Chem. B.* **2000**, *104*, 292−301.
(48) Luan, Z.; Cheng, C.-F.; Zhou, W.; Klinowski, J. *J. Phys. Chem.* **1995**, *99*, 1018−1024.
(49) Matsumoto, A.; Misran, H.; Tsutsumi, K. *Langmuir* **2004**, *20*, 7139−7145.
(50) Ravikovitch, P. I.; Wei, D.; Chueh, W. T.; Haller, G. L.; Neimark, A. V. *J. Phys. Chem. B* **1997**, *101*, 3671−3679.

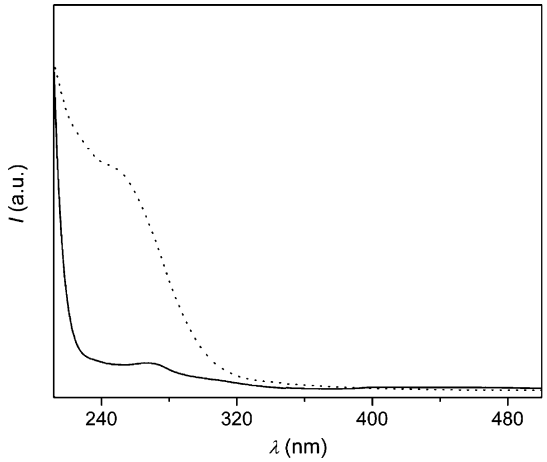

Figure 6. Diffuse-reflectance UV/vis spectra of UreaMS (full line) and Fe−UreaMS (dotted line).

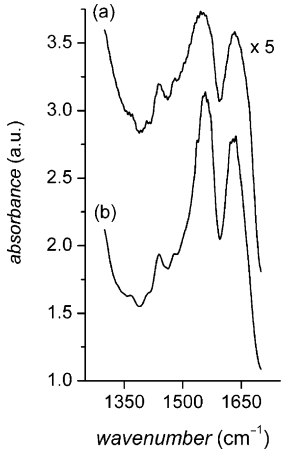

Figure 7. FT-IR spectra of (a) UreaMS and (b) Fe−UreaMS recorded at 373 K.

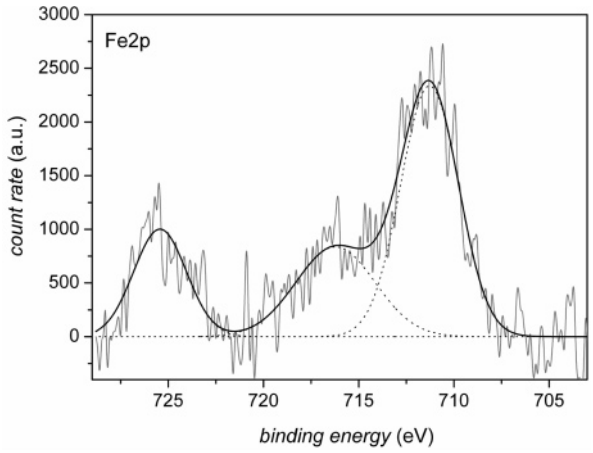

Figure 8. Fe 2p XPS graph for Fe−UreaMS.

potential re-usability of the material was demonstrated by washing Fe(III)-loaded UreaMS with 0.1 M HCl and copious amounts of water. The use of the thus-obtained material in a second Fe(III) adsorption experiment led to a nonoptimized value of 65% of the initial Fe(III) loading.

In a further experiment the material was loaded with Fe(III) to its maximum extent by treatment with a higher concentrated aqueous solution of $FeCl_3$ (40 mM), resulting in Fe−UreaMS. Chemical analysis for iron yielded an adsorption capacity of 10.4 mg (0.19 mmol) per 1 g of UreaMS. A recently published material with large pores and covalently anchored pyoverdin ligands was shown to sequester highly selectively Fe(III) from aqueous solutions.[51] However, the reported capacity for Fe(III) uptake is considerably lower than that for UreaMS (0.033 mmol of Fe per 1 g of solid versus 0.19 mmol of Fe per 1 g of UreaMS). Apparently, the number of organic functionalities in UreaMS is higher than what is usually obtained by postsynthetic modification of silica materials. Noteworthy, not all urea units in UreaMS, but approximately one of every six, bind Fe(III). In other words, we reach already a saturation limit in terms of the urea/Fe(III) ratio, which would appear to make the application of a PMO with a much higher urea content rather uneconomical.

Fe−UreaMS was characterized by diffuse-reflectance UV/vis spectroscopy (cf. Figure 6). The spectrum exhibited a strong shoulder at ca. 250 nm with a long tailing up to 400 nm. These spectral features were not present in the unloaded UreaMS, as shown in the same figure. Therefore, the new absorption band was ascribed to a Fe(III)−urea complex.

Characterization of unloaded UreaMS by means of FT-IR spectroscopy revealed amide bands with maxima at 1634 cm^{-1} (amide I) and 1550 cm^{-1} (amide II), typical for urea (cf. Figure 7).[52] The amide I band receives its major contribution from the C═O stretching mode and is sensitive to hydrogen bonding. The large range of frequencies (ca. 100 cm^{-1}) covered by the band suggests that more than one contribution is present, probably resulting from hydrogen-bonded and non-hydrogen-bonded carbonyls. Hydrogen bonding with silanol groups can, thus, not be excluded. The amide II band has its maximum at 1550 cm^{-1}, typical for noncyclic secondary amides with trans configuration between the N−H and the C═O groups, where the N−H bending and the C−N stretching modes interact.[53]

The FT-IR spectrum of Fe−UreaMS (at 373 K under vacuum) was also recorded (cf. Figure 7) and revealed urea-typical amide bands [1629 cm^{-1} (ν_{CO}, amide I) and 1558 cm^{-1} (δ_{NH}, amide II)] but slightly shifted as compared to the unloaded UreaMS: −5 cm^{-1} and +8 cm^{-1} for amides I and II, respectively. Two different binding modes for Fe(III) with urea can be imagined: either via NH or via the C═O oxygen. An earlier detailed investigation of various cation−urea complexes, among them Fe(III)−urea, revealed that Fe(III) binds preferentially to the carbonyl oxygen.[54] However, for this binding mode no strong shifts of the corresponding IR bands have been observed, akin to the situation in UreaMS. Recently, for Fe(III)-doped diureasils the dominant role of the urea C═O oxygen in the binding of the metal cation has also been emphasized.[55] Therefore, a similar binding of Fe(III) is assumed for UreaMS.

(51) Renard, G.; Mureseanu, M.; Galarneau, A.; Lerner, D. A.; Brunel, D. *New J. Chem.* **2005**, *29*, 912−918.
(52) Kim, J. T. *J. Korean Chem. Soc.* **1970**, *14*, 147−153.
(53) de Zea Bermudez, V.; Carlos, L. D.; Alcácer, L. *Chem. Mater.* **1999**, *11*, 569−580.
(54) Penland, R. B.; Mizushima, S.; Curran, C.; Quagliano, J. V. *J. Am. Chem. Soc.* **1957**, *79*, 1575−1578.
(55) Silva, N. J. O.; Amaral, V. S.; de Zea Bermudez, V.; Nunes, S. C.; Ostrovskii, D.; Rocha, J.; Carlos, L. D. *J. Mater. Chem.* **2005**, *15*, 484−490.

Finally, XPS analysis of the Fe−UreaMS (cf. Figure 8) revealed two peaks corresponding to Fe $2p_{3/2}$ and Fe $2p_{1/2}$ at 711.2 and 725.3 eV, respectively, and a broad satellite peak around 716.3 eV. These binding energies are characteristic of Fe(III) cations,[56] confirming the preservation of the oxidation state +3 for the iron in the material and the absence of iron oxide clusters in UreaMS.

Conclusions

A novel urea-containing mesoporous silica (UreaMS) was prepared and characterized. The material possesses one urea group per ca. 13−16 Si atoms. ^{29}Si MAS NMR and XPS studies support a high degree of condensation and the uniform distribution of the urea within the silica framework. In comparison with previously reported materials for iron adsorption, i.e., urea-containing organic−inorganic sol−gel materials (ureasils) and a large-pore silica with an anchored Fe(III) binding ligand, UreaMS has several advantages: (a) a periodic mesoporosity and a larger specific surface area as compared to ureasils and (b) a higher metal binding capacity than the large-pore material and no complications due to pore blocking. One of every six urea functions was found to participate in Fe(III) adsorption, which means that materials with higher organic content (e.g., PMOs) would be economically unreasonable in this case. The combination of PXRD and N_2 adsorption isotherm measurements proved that a hexagonally ordered mesoporous material was obtained. The high efficiency of the material for the adsorption of Fe(III) was demonstrated.

Acknowledgment. Financial support from the Spanish Ministry of Education and Science (Project CTQ 2006-6854, Ramón y Cajal grant for U.P.), the Generalitat Valenciana (Grupos 03-020), and the COST activity D29 (Sustainable/Green Chemistry and Chemical Technology) is gratefully acknowledged. Dr. Carlos Sá performed the XPS measurements at the Centro de Materiais da Universidade do Porto (CEMUP). The authors thank Dr. António Labrincha (ESTG-IPVC) for the TGA measurements.

CM061287N

(56) Kim, Y. J.; Park, C. R. *Inorg. Chem.* **2002**, *41*, 6211−6216.